Phytopathology Research

RESEARCH

Open Access

Extra-large G proteins regulate disease resistance by directly coupling to immune receptors in *Nicotiana benthamiana*

Yixin Li[1], Qian Zhang[1], Lijing Gong[2], Jun Kong[2], Xiaodan Wang[1], Guangyuan Xu[1], Xujun Chen[1], Daolong Dou[1,3] and Xiangxiu Liang[1,2*]

Abstract

Heterotrimeric G proteins, comprising Gα, Gβ, and Gγ subunits, are key regulators of eukaryotic intracellular signaling. Extra-large G (XLG) proteins are a subfamily of plant-specific Gα proteins interacting with plasma membrane-localized receptors to regulate multiple biological processes. The *Nicotiana benthamiana* genome encodes seven XLG proteins, NbXLG1–7, whose functions in disease resistance and underlying mechanisms are unknown. In this study, we silenced all the seven genes and found that disease susceptibility was enhanced when both *NbXLG3* and *NbXLG5* or *NbXLG4* was silenced. Then, we generated *N. benthamiana xlg3xlg5* double- and *xlg4* single-mutant lines using the CRISPR-Cas9 approach. All the mutants showed reduced resistance to the bacterial pathogen *Pseudomonas syringae* pv. *tomato* DC3000, the fungal pathogen *Sclerotinia sclerotiorum*, and a series of oomycete pathogens, including *Phytophthora capsici*, *Phytophthora infestans*, and *Phytophthora parasitica*. We further demonstrated that NbXLG3/4/5 positively regulated microbial pattern-induced reactive oxygen species burst and defense gene expression by directly coupling to the tested plant immune receptors. In addition, we examined the role of NbXLG3/4/5 in abiotic stress tolerance and observed that NbXLG3 and NbXLG5 negatively regulated plant resistance to high-salt, mannitol, and PEG. Our study demonstrates the possible role of NbXLG3/4/5 in response to biotic and abiotic stresses and provides insights for the improvement of plant resistance to environmental changes.

Keywords: NbXLG, Immune response, Plant resistance, Abiotic stress

Background

The heterotrimeric G protein complex, composed of α, β, and γ subunits, is one of the most important signal transducers in eukaryotic cells (Pandey 2019). G proteins are key regulators of extracellular signal transduction. In animals and fungi, the Gα subunit is directly coupled to seven-transmembrane G protein coupled receptors (GPCRs) that perceive extracellular signals through the ectodomains. GPCRs transmit these extracellular signals to Gαs, causing Gαs to exchange GDP for GTP, resulting in the activation of G protein heterotrimers. An activated Gα separates from Gβγ and they each function on their downstream targets (also known as G protein effectors) to transduce and amplify signals (Oldham and Hamm 2008). In plants, there is mounting evidence that G proteins are directly coupled to single-transmembrane receptor-like proteins (RLPs) and receptor kinases (RKs) to transduce extracellular signals to downstream effectors (Bommert et al. 2013; Choudhury and Pandey 2015; Liang et al. 2016; Yu et al. 2018; Zhao et al. 2022). Animals have a much larger number of G protein subunits that can form multiple heterotrimer combinations. For example, humans have 23 Gαs, 5 Gβs, and 12 Gγs.

*Correspondence: liangxiangxiu@scau.edu.cn

[1] College of Plant Protection, China Agricultural University, Beijing 100193, China
Full list of author information is available at the end of the article

© The Author(s) 2022. **Open Access** This article is licensed under a Creative Commons Attribution 4.0 International License, which permits use, sharing, adaptation, distribution and reproduction in any medium or format, as long as you give appropriate credit to the original author(s) and the source, provide a link to the Creative Commons licence, and indicate if changes were made. The images or other third party material in this article are included in the article's Creative Commons licence, unless indicated otherwise in a credit line to the material. If material is not included in the article's Creative Commons licence and your intended use is not permitted by statutory regulation or exceeds the permitted use, you will need to obtain permission directly from the copyright holder. To view a copy of this licence, visit http://creativecommons.org/licenses/by/4.0/.

In contrast, plants have fewer G protein subunits. *Arabidopsis* and rice have only one canonical Gα subunit, three extra-large G (XLG) proteins, one Gβ subunit, and three and five Gγ subunits, respectively (Stateczny et al. 2016). XLG proteins are widespread in all higher plants and contain a C-terminal Gα-like domain and an N-terminal extension (Lee and Assmann 1999).

Plant G proteins are essential for many biological processes. *Arabidopsis* G proteins have been reported to regulate growth and development and respond to multiple hormones, abiotic stresses, and plant immune responses (Urano et al. 2016; Pandey 2019). Mutation of the *Gα* or *Gβ* genes in monocots (rice and maize) leads to a dwarf-like or lethal phenotype (Fujisawa et al. 1999; Ueguchi-Tanaka et al. 2000; Utsunomiya et al. 2012; Bommert et al. 2013). Dense and erect panicle 1 (DEP1), a rice Gγ protein, regulates erectness, panicle branching, and nitrogen assimilation (Huang et al. 2009; Sun et al. 2014). Rice Gγ protein grain size 3 (GS3) has been identified as the major allele controlling rice grain size (Fan et al. 2006). Another Gγ protein, RGG2, has been reported to be a negative regulator of grain size and yield (Miao et al. 2019). CT2, a Gα protein in maize, interacts with the CLAVATA receptor and regulates shoot apical meristem development (Bommert et al. 2013).

Recently, XLG proteins have been considered plant-specific Gα subunits, which greatly increase the functional diversity of plant G proteins. *Arabidopsis* XLG proteins are required to respond to hormonal and abiotic stresses (Ding et al. 2008; Pandey et al. 2008). The rice genome encodes three XLG proteins required for modeling yield-related traits, including plant height, panicle length, tiller number, and 1000-grain weight (Zhao et al. 2022). Maize XLGs have been reported to regulate shoot apical meristem development, and mutations in all three *ZmXLGs* are lethal (Wu et al. 2018). XLGs also play important roles in plant resistance to phytopathogens and in regulating immune signals (Zhu et al. 2009; Liu et al. 2013; Maruta et al. 2015; Liang et al. 2016, 2018; Ma et al. 2022; Wang et al. 2022; Zhao et al. 2022). Plant cells can recognize conserved microbial features, termed microbial patterns, using surface-localized pattern-recognition receptors (PRRs) to sense the invasion of microbial pathogens. Perception of microbial patterns by PRRs causes the activation of pattern-triggered immunity (PTI), which includes the transient influx of calcium, burst of reactive oxygen species (ROS), activation of MAP kinases, and transcriptional reprogramming (DeFalco and Zipfel 2021). The *Arabidopsis* receptor-like kinase (RLK) protein FLS2 recognizes bacterial flagellin (or flg22 epitope) in the presence of the co-receptor BAK1 (Chinchilla et al. 2006, 2007). The *Arabidopsis* RLK proteins LYK4/5 and CERK1 form a complex that recognizes fungal cell wall-derived chitin (Cao et al. 2014). We have previously shown that XLG2 and XLG3 are directly coupled to the FLS2 receptor to regulate flg22-induced immune signaling (Liang et al. 2016). Zhao et al. (2022) showed that rice XLG proteins regulate microbial pattern-induced immune activation and play different roles in plant resistance to bacterial and fungal infections (Zhao et al. 2022).

In the present study, we showed that the *N. benthamiana* genome encodes seven XLG proteins (NbXLGs), of which NbXLG3, NbXLG4, and NbXLG5 are required for plant resistance against bacterial and fungal pathogens. We further demonstrated that these three NbXLGs contribute to plant oomycete pathogen resistance. In addition, NbXLG3, NbXLG4, and NbXLG5 were found to regulate microbial pattern-induced immunity by interacting with PRRs. We also showed that NbXLG3 and NbXLG5, but not NbXLG4, negatively regulate plant resistance to abiotic stresses. Overall, our study revealed the biological functions of NbXLG proteins and how they can be used to potentially improve plant resistance to biotic and abiotic stresses.

Results

Identification of the *NbXLGs* involved in plant immunity

XLG proteins have been reported to regulate plant immunity, growth, and development in the model plant *Arabidopsis*. However, the functions of XLG proteins in *Solanaceae* plants have not been studied. We showed that there are 5–7 XLGs in *N. benthamiana*, *Solanum lycopersicum*, and *Solanum tuberosum* (Additional file 1: Figure S1 and Additional file 2: Table S1). Although most XLGs are grouped with *Arabidopsis* XLGs, a clade of *Solanaceae* XLGs cannot be grouped with *Arabidopsis* XLGs (Additional file 1: Figure S1). The *N. benthamiana* genome encodes one canonical Gα (NbGα) and seven XLG proteins, NbXLG1 (Niben101Scf00372g05021), NbXLG2 (Niben101Scf04286g01030), NbXLG3 (Niben101Scf01202g02006), NbXLG4 (Niben101Scf05674g05014), NbXLG5 (Niben101Scf06100g02001), NbXLG6 (Niben101Scf04383g01013), and NbXLG7 (Niben101Scf01249g03025) (Fig. 1a and Additional file 2: Table S1).

To determine the role of NbXLGs in plant immunity, we silenced *NbXLG* genes using virus-induced gene silencing (VIGS). Based on the phylogenetic tree, we constructed four VIGS vectors targeting *NbXLG1,6*, *NbXLG2,7*, *NbXLG3,5*, and *NbXLG4*. We then challenged the plants with *S. sclerotiorum* and examined lesion development one day later. *NbXLG3,5*- and *NbXLG4*-silenced plants exhibited significantly enhanced susceptibility to *S. sclerotiorum* (Fig. 1b). We then examined

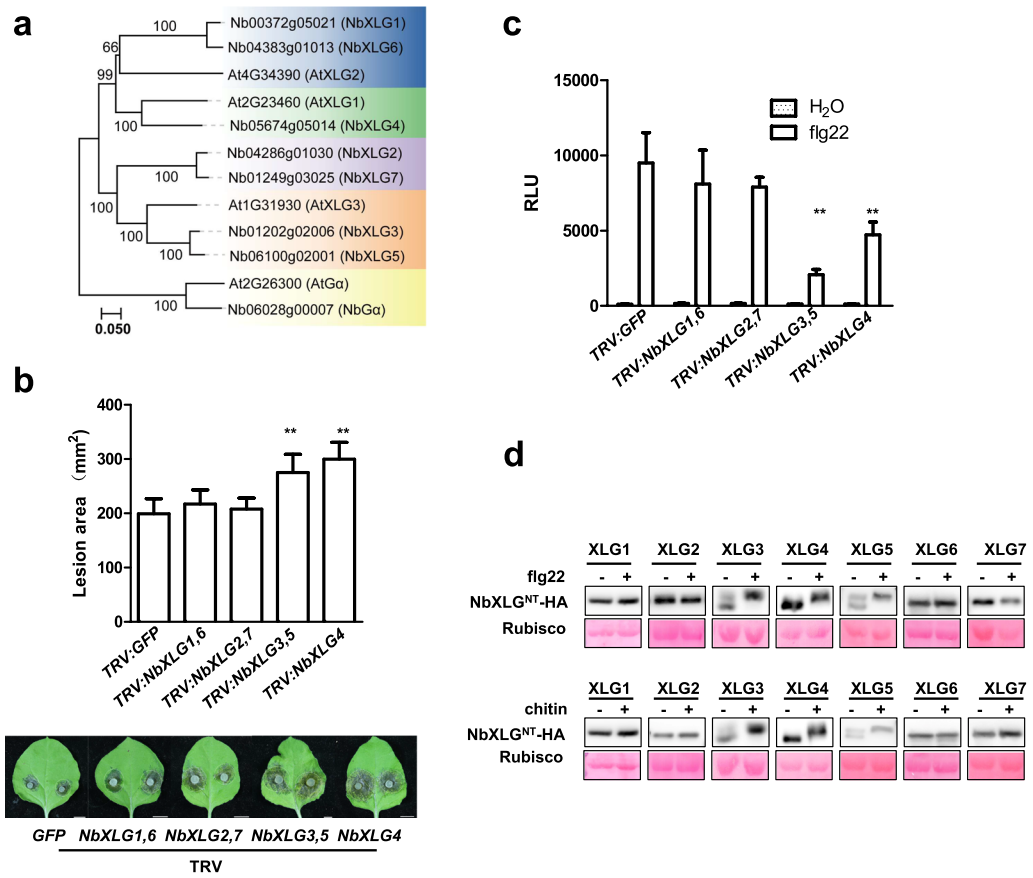

Fig. 1 Analyzation of XLG proteins in *Nicotiana benthamiana*. **a** Phylogenetic analysis of Gα proteins from *N. benthamiana* and *Arabidopsis*. **b** Silencing of *NbXLG3,5* or *NbXLG4* leads to enhanced susceptibility to *Sclerotinia sclerotiorum*. The indicated *NbXLG* genes were silenced by virus-induced gene silencing (VIGS). The plants were inoculated with *S. sclerotiorum* and photographed under UV light at 24 h post-inoculation (hpi). The lesion areas were measured and calculated (mean ± SD, n ≥ 6, student's *t* test, **significant difference at $P < 0.01$). Scale bar, 1 cm. **c** Silencing of *NbXLG3,5* or *NbXLG4* leads to compromised flg22-induced ROS production. The indicated *NbXLG*-silenced plants were subjected to flg22-induced ROS examination (mean ± SD, n ≥ 6, student's *t* test, **significant difference at $P < 0.01$). RLU, relative luminescence units. **d** Flg22 and chitin induce protein band shift of NbXLG3, NbXLG4, and NbXLG5 in the N-terminus. The N-terminal ~ 200 amino acid of NbXLGs were transiently expressed in *N. benthamiana* for 2 days, infiltrated with 1 μM flg22, or 200 μg/mL chitin for 10 min, and protein band shift was examined by anti-HA immunoblots

flg22-induced ROS burst, a typical assay for measuring microbial pattern-induced immunity, in *NbXLG*-silenced plants. The results showed that ROS production was slightly reduced in *NbXLG1,6*- or *NbXLG2,7*-silenced plants but severely reduced in *NbXLG3,5*- or *NbXLG4*-silenced plants (Fig. 1c). Quantitative real-time PCR (qPCR) analysis showed that all the target *NbXLG* genes were successfully silenced via VIGS (Additional file 1: Figure S2a, b). We previously showed that immune-related *Arabidopsis* XLGs are phosphorylated upon microbial pattern treatment at the N-terminus (Liang et al. 2016; Ma et al. 2022). Thus, we transiently expressed the N-terminus of approximately 200 amino acids of NbXLGs in *N. benthamiana* and examined the flg22-induced band shift by western blotting to detect protein phosphorylation. Consistent with the *S. sclerotiorum* infection and flg22-induced ROS assays, the N-terminus of NbXLG3, NbXLG4, and NbXLG5 showed a prominent band shift in the SDS-PAGE gel upon treatment with bacterial pattern flg22 or fungal pattern chitin (Fig. 1d). These results indicate that NbXLG3, NbXLG4, and NbXLG5 are involved in plant immunity.

Construction of *Nbxlg3,5* and *Nbxlg4* knockout mutants

To further analyze the roles of *NbXLG3*, *NbXLG4*, and *NbXLG5* in plant immunity, we generated *Nbxlg* knockout lines using the CRISPR-Cas9 approach. *NbXLG3* and *NbXLG5* showed high sequence identities and similarities. Thus, we designed two guide RNAs (gRNAs) targeting *NbXLG3* and *NbXLG5* and cloned them into the

pHEE401E vector (Wang et al. 2015) (Fig. 2a). In addition, we designed two gRNAs targeting the N-terminus of *NbXLG4* (Fig. 2a). After screening of transgenic lines, we obtained two mutant alleles for each gene. We generated a 61 bp deletion in *NbXLG3* and a 1 bp deletion in *NbXLG5* (*Nbxlg3,5*-L1), a 1 bp insertion in *NbXLG3* and a 2 bp deletion in *NbXLG5* (*Nbxlg3,5*-L2), a 4 bp deletion in *NbXLG4* (*Nbxlg4*-L1), and a 33 bp deletion in *NbXLG4* (*Nbxlg4*-L2) (Fig. 2a). PCR and sequencing confirmed the gene editing results (Additional file 1: Figure S3). As shown in Fig. 2b, none of the *Nbxlg* knockout mutants showed visible severe growth and development defects (Fig. 2b). Therefore, we selected two independent homozygous lines without Cas9 expression (Cas9-free)

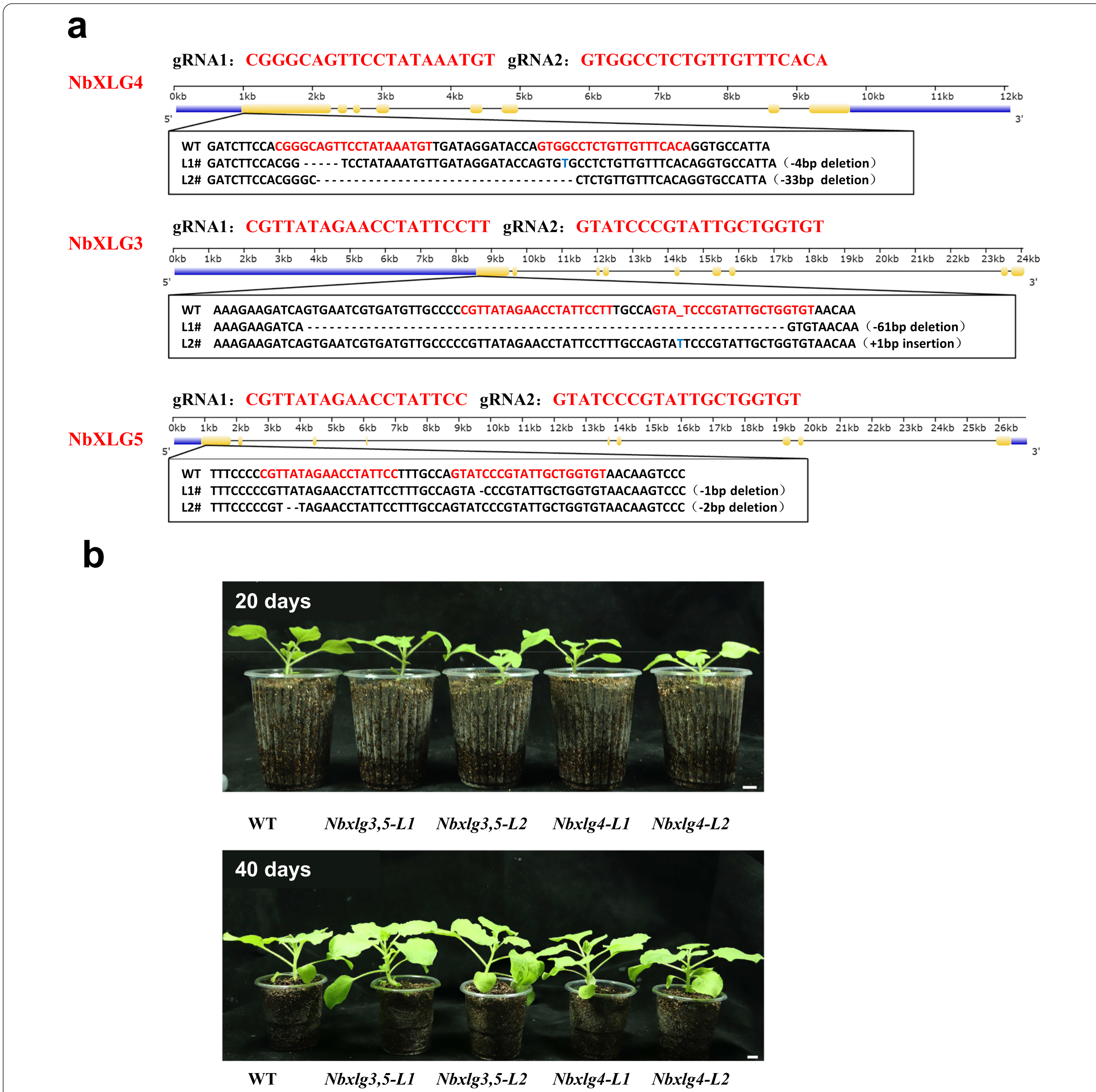

Fig. 2 Generation of *Nbxlg3,5*- or *Nbxlg4*-knockout mutants. **a** Knocking out of *NbXLG3,5* or *NbXLG4* via CRISPR/Cas9 approach. In the schematic map, the exons, introns, and UTRs are indicated as yellow boxes, lines, and bule boxes, respectively. The gRNA sequences and gene editing results are listed in the diagram. The DNA-sequencing chromatograms are shown in Additional file 1: Figure S3. **b** Morphologic phenotypes of 20- and 40- days-old *NbXLG3,5* and *Nbxlg4* mutant plants. Bar, 1 cm

for each transgene for further studies (Additional file 1: Figure S4a–d).

NbXLG3/4/5 are required for plant resistance to bacterial and fungal pathogens

To evaluate the function of NbXLG3/5 and NbXLG4 in plant resistance, we examined plant resistance to the bacterial pathogen *Pseudomonas syringae* pv. *tomato* DC3000 (*Pst* DC3000) and the fungal pathogen *S. sclerotiorum*. All *Nbxlg3,5* (*Nbxlg3,5*-L1 and L2) and *Nbxlg4* (*Nbxlg4*-L1 and L2) mutant lines showed significantly reduced resistance to *Pst* DC3000 (Fig. 3a). We then introduced *Pst* DC3000 *hrcC*$^{-}$, a mutant strain defective in secreting virulence effectors and used to measure microbial pattern-induced immune responses. All *Nbxlg3,5* and *Nbxlg4* mutants showed enhanced susceptibility to *Pst hrcC*$^{-}$ infection (Fig. 3b), suggesting a positive role for NbXLG3/5 and NbXLG4 in microbial pattern-triggered immunity. Next, we infected *Nbxlg* mutants with the fungal pathogen *S. sclerotiorum*. We found that *Nbxlg3,5* and *Nbxlg4* mutants exhibited much larger lesions than the wild-type (WT) plants (Fig. 3c), consistent with the result of *S. sclerotiorum* infection assay in *NbXLG*-silenced plants (Fig. 1b). Our results show that NbXLG3/5 and NbXLG4 positively regulate plant resistance against bacterial and fungal pathogens.

NbXLG3/4/5 are required for plant resistance to oomycete pathogens

We next investigated the role of NbXLG proteins in plant resistance to oomycete pathogens, which has not been studied. We inoculated the WT, *Nbxlg3,5*, and *Nbxlg4* plants with oomycete pathogens, including *P. capsici*, *P. infestans*, and *P. parasitica*. Knocking out *NbXLG3,5* or *NbXLG4* substantially reduced plant resistance to *P. capsici* (Fig. 4a). In addition, the mutant lines developed a much larger lesion than the WT plants upon *P. capsici* infection (Fig. 4a). Similarly, all *Nbxlg3,5* and *Nbxlg4* mutant lines showed enhanced susceptibility to *P. infestans* and *P. parasitica* (Fig. 4b, c). The lesions in the *Nbxlg3,5* and *Nbxlg4* mutant lines were much larger than those in the WT plants upon *P. infestans* or *P. parasitica* infection (Fig. 4b, c). Altogether, our findings revealed that NbXLG3, NbXLG4, and NbXLG5 play pivotal roles in plant resistance to oomycete pathogens.

NbXLGs positively regulate microbial patterns-induced immunity by coupling to plant immune receptors

Pattern-triggered immunity (PTI) confers broad resistance to most microbes. Considering NbXLG3/5 and NbXLG4 are required for plant resistance to multiple pathogens, we deduced that NbXLG3/5 and NbXLG4 are required for PTI. Microbial pattern-triggered ROS burst is a specific assay for examining PTI activation, we thus treated *N. benthamiana* plants with bacteria-derived flg22 or fungal-derived chitin and examined ROS production. All *Nbxlg3,5* and *Nbxlg4* mutant lines

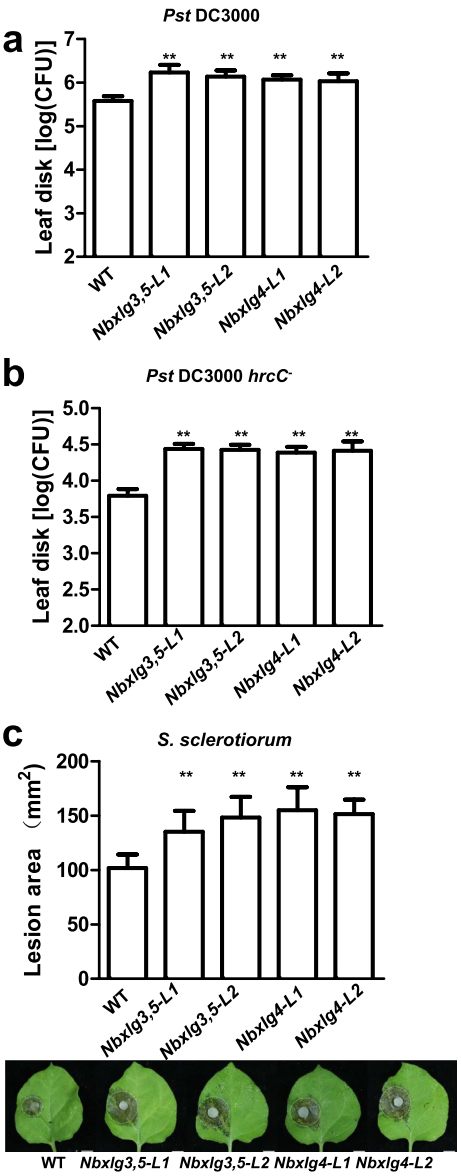

Fig. 3 *Nbxlg3,5* and *Nbxlg4* mutant plants have reduced resistance to bacterial and fungal pathogens. **a**, **b** *Nbxlg3,5* and *Nbxlg4* mutants showed enhanced disease susceptibility to *Pst* DC3000 (**a**) and *Pst* DC3000 *hrcC*$^{-}$ (**b**). The plants were infiltrated with the indicated *Pst* strains, and in planta bacterial titers were determined at 3 days post-inoculation (dpi) (mean ± SD, n ≥ 6, student's *t*-test, **significant difference at $P < 0.01$). **c** *Nbxlg3,5* and *Nbxlg4* mutants showed enhanced disease susceptibility to *Sclerotinia sclerotiorum*. The leaves were inoculated with *S. sclerotiorum* and photographed at 1 dpi, and the lesion areas were measured (mean ± SD, n ≥ 8, student's *t* test, **significant difference at $P < 0.01$). Scale bar, 1 cm

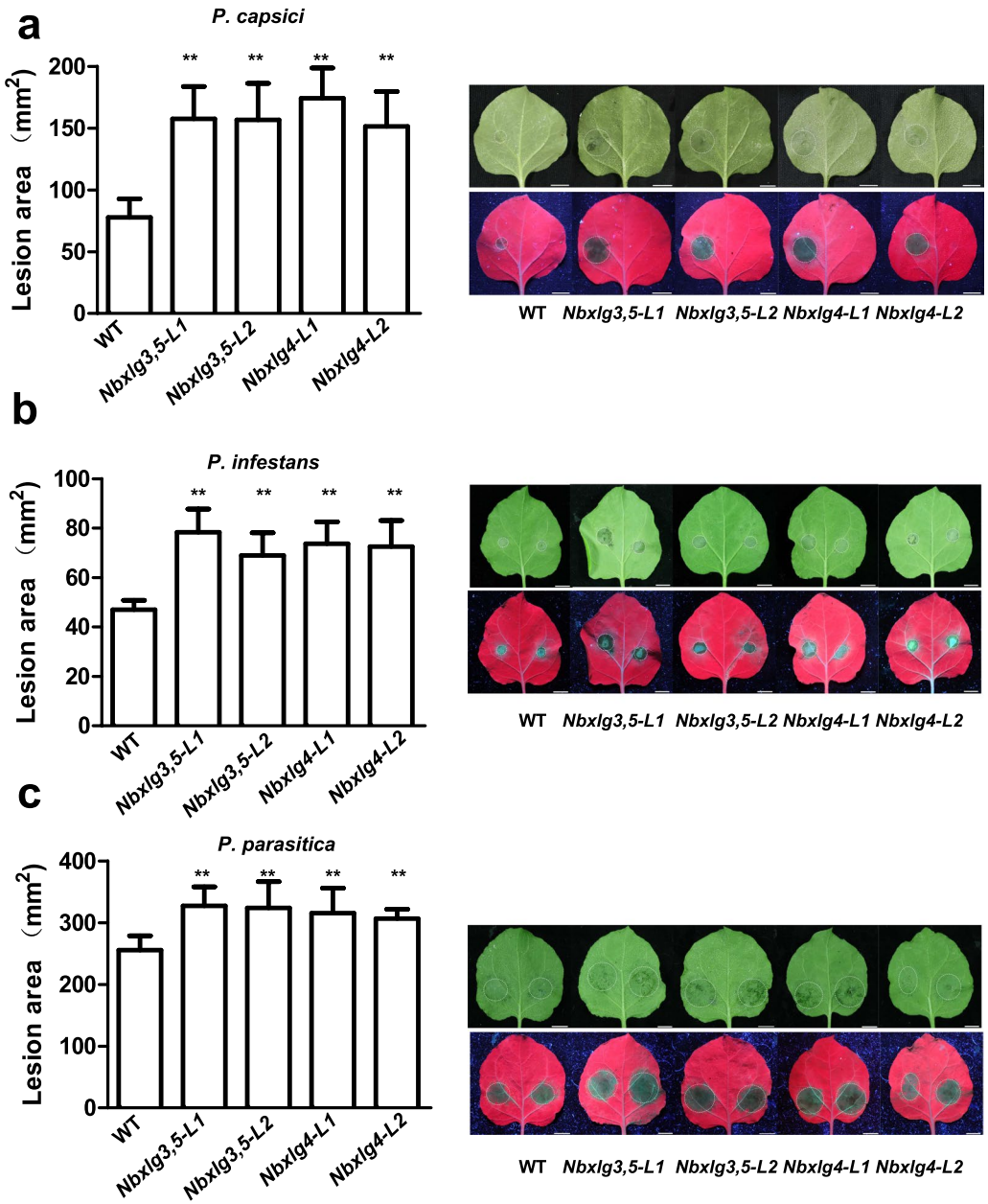

Fig. 4 *Nbxlg3,5* and *Nbxlg4* mutant plants have reduced resistance to oomycete pathogens. The WT, *Nbxlg3,5 and Nbxlg4* plants were inoculated with *Phytophthora capsici* (**a**), *Phytophthora infestans* (**b**), or *Phytophthora parasitica* (**c**). Photographs were taken under UV light and lesion areas were measured at 36–48 hpi, 7 dpi, and 60 hpi for *P. capsici*, *P. infestans*, and *P. parasitica*, respectively (mean ± SD, n ≥ 8, student's *t* test, **significant difference at $P < 0.01$). Scale bar, 1 cm

displayed significantly reduced flg22- and chitin-induced ROS bursts compared to the WT plants (Fig. 5a, b). We next checked defense gene expression in different *Nbxlg* mutants upon flg22 or chitin treatment. We examined the expression of *ACRE31* and *PTI5*, and found they were highly induced by flg22 and chitin at 3 h after treatment (Fig. 5c, d). However, the *Nbxlg3,5* and *Nbxlg4* mutant lines showed a significantly compromised expression of *ACRE31* and *PTI5* upon flg22 or chitin treatment compared with the WT plants (Fig. 5c, d). The microbial pattern-induced phosphorylation of MAPKs is another typical assay for examining PTI. Therefore, we examined flg22- or chitin-induced activation of MAPKs in *Nbxlg3,5* and *Nbxlg4* mutants using anti-p-ERK immunoblots, and

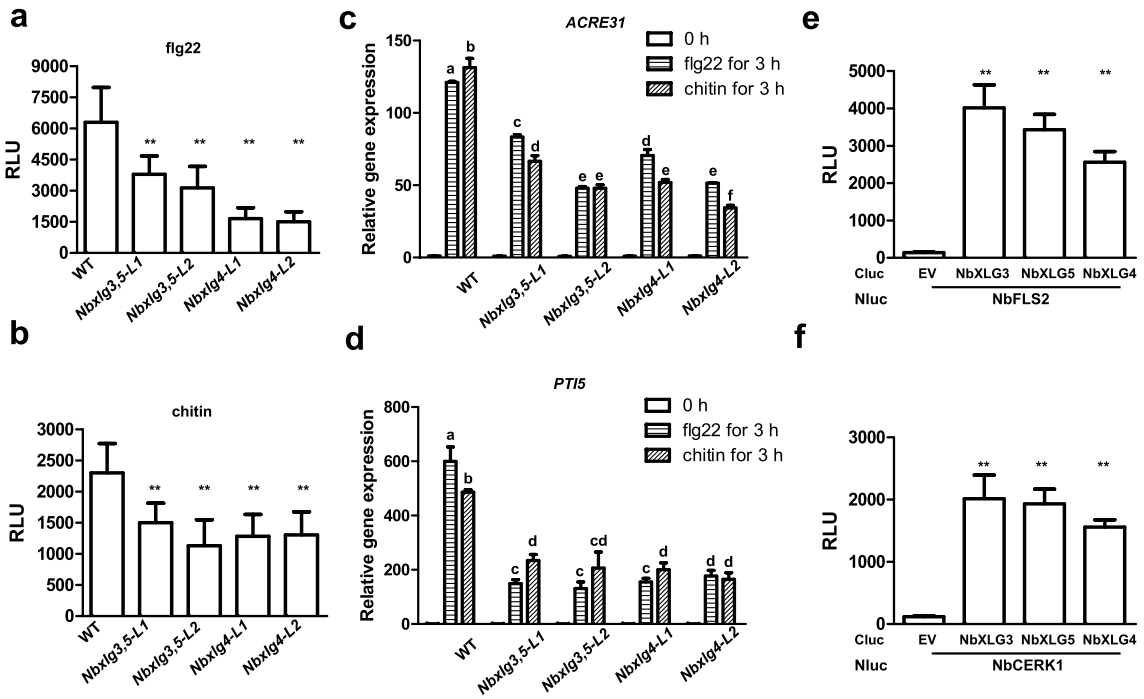

Fig. 5 NbXLG3, NbXLG4, and NbXLG5 regulate flg22- or chitin-induced ROS and defence gene expression by coupling to plant immune receptors. **a**, **b** The *Nbxlg3,5* and *Nbxlg4* mutant lines showed significantly reduced ROS burst upon flg22 (**a**) or chitin (**b**) treatment. The indicated plants were examined for flg22- or chitin-induced ROS burst and the peak RLU value were recorded (mean ± SD, n ≥ 6, student's *t* test, **significant difference at $P < 0.01$). **c**, **d** Flg22- or chitin- induced expression of defence marker gene *ACRE31* and *PTI5* are compromised in *Nbxlg3,5* and *Nbxlg4* mutant lines (Mean ± SD; student's *t* test, **significant difference at $P < 0.01$.). **e**, **f** NbXLG3/5 and NbXLG4 interact with NbFLS2 (**e**) and NbCERK1(**f**). The indicated constructs were transiently expressed in *Nicotiana benthamiana* and protein interactions were examined by luciferase complementation image (LCI) assays (mean ± SD; n ≥ 6, student's *t* test, **significant difference at $P < 0.01$). In **a**, **b**, **e**, and **f**, RLU indicates relative luminescence units

found that flg22- or chitin-induced activation of MAPKs were not affected by mutations in *NbXLG3/5* or *NbXLG4* (Additional file 1: Figure S5a, b).

To confirm that compromised PTI activation was caused by mutations in *NbXLG3/5* or *NbXLG4*, we transiently expressed NbXLG3 and NbXLG4 in *Nbxlg3,5* and *Nbxlg4* mutants, respectively, and examined flg22-induced ROS production. We noticed that transient expression of NbXLG3 could fully restore the reduced ROS levels in *Nbxlg3,5* (Additional file 1: Figure S6a). Similarly, NbXLG4 expression restored the *Nbxlg4* defect in flg22-induced ROS (Additional file 1: Figure S6b). These results confirm the role of NbXLG3/5 and NbXLG4 in plant immunity. Notably, the expression of the *Arabidopsis* XLG1, XLG2 or XLG3 cannot restore the reduced flg22-induced ROS burst caused by the mutation of *NbXLG3/5* and *NbXLG4* (Additional file 1: Figure S6a–d).

We have previously shown that AtXLGs form complexes with Gβγ dimers and are directly coupled to the plant immune receptor complex. Luciferase complementation image (LCI) assays showed that NbXLG3/5 and NbXLG4 interacted with NbGβ (Additional file 1: Figure S7a). Co-IP assays showed that NbXLG3 and NbXLG4 interacted with NbGβ (Additional file 1: Figure S7b). These results indicate that NbXLGs can form heterotrimers with Gβγ dimers. Next, we showed that NbXLG3, NbXLG4, and NbXLG5 interacted with the NbFLS2 and NbCERK1 receptors by LCI assays (Fig. 5e, f). We further confirmed NbXLG3-NbFLS2 and NbXLG4-NbFLS2 interactions using Co-IP assays (Additional file 1: Figure S7c). Collectively, we demonstrated that NbXLG3, NbXLG5, and NbXLG4, coupled with immune receptors to regulate pattern-triggered immunity.

NbXLG3/5 negatively regulates plant abiotic stresses

Arabidopsis XLG proteins have been reported to play a positive role in response to abiotic stresses (osmotic and salt stresses) and hormones (ABA and ET) (Ding et al. 2008; Urano et al. 2016). Therefore, we analyzed the roles of NbXLG3, NbXLG4, and NbXLG5 in high-salt or osmotic stress tolerance and examined the root length under different concentrations of NaCl, mannitol, and polyethylene glycol (PEG). *Nbxlg3,5*-L1 and *Nbxlg3,5*-L2 mutant lines showed significantly enhanced

resistance to 200 mM NaCl but normal resistance to 250 mM NaCl (Fig. 6a and Additional file 1: Figure S8). Compared to the WT, the *Nbxlg3,5*-L1 and *Nbxlg3,5*-L2 mutants showed enhanced resistance to mannitol (300 and 400 mM) and PEG (2.5% and 5%) (Fig. 6a and Additional file 1: Figure S8), suggesting a negative role of NbXLG3/5 in osmotic stress tolerance. However, the *Nbxlg4*-L1 and *Nbxlg4*-L2 mutant lines showed normal resistance to NaCl, mannitol, and PEG stresses, indicating that NbXLG4 is not required for salt or osmotic stress (Fig. 6b and Additional file 1: Figure S9). Altogether, we demonstrated that NbXLG3 and NbXLG5 play a negative role in plant response to abiotic stresses.

Discussion

Heterotrimeric G proteins have been well studied regarding their functions, regulatory mechanisms, and structures in animals and fungi. The animal working model for G proteins has been established for years and is considered the most well-understood pathway. Over the last decade, plant heterotrimeric G proteins have been extensively studied, and the similarities and differences between plant and animal G proteins are actively being discovered. The plant genome encodes several G protein subunits and the theoretical number of heterotrimer combinations is limited. However, the discovery of XLG proteins, a subfamily of plant-specific Gα proteins, has greatly increased the number of heterotrimers and the functional diversity of plant G proteins. To date, most studies on XLG proteins have been conducted in *Arabidopsis*. However, XLG proteins in *Solanaceae* plants, such as *N. benthamiana*, have not been studied.

Bioinformatics analysis revealed that *Solanaceae* plants have more XLG proteins than *Arabidopsis* plants. There are five XLGs in tomato and potato plants, while seven XLGs are present in *N. benthamiana* (Additional file 1: Figure S1). We noticed that a subfamily of XLG proteins in *Solanaceae* plants did not cluster with AtXLGs, suggesting that they might possess specific functions that differ from those of AtXLGs. We silenced *NbXLG*s via VIGS and showed that *NbXLG3/5* and *NbXLG4* contribute to *S. sclerotiorum* resistance and flg22-induced ROS production (Fig. 1b, c). These results suggest a role for NbXLG3/5 and NbXLG4 in plant immunity. We previously reported that AtXLG2 and AtXLG3 are phosphorylated at the N-terminus following flg22 treatment (Liang et al. 2016). In this study, we showed that flg22 and chitin induced N-terminal phosphorylation of NbXLG3, NbXLG4, and NbXLG5 (Fig. 1d), further supporting their role in plant immunity. The specific phosphosites of these three NbXLGs and their functions remain unknown. It would be interesting to study whether the phosphosites of XLGs are conserved in *Arabidopsis* and *N. benthamiana*.

To better analyze the functions of NbXLG3/5 and NbXLG4, we constructed two independent mutant lines, Nb*xlg3,5* and *Nbxlg4*, using the CRISPR-Cas9 approach. Notably, *Nbxlg4*-L2 possesses a 33-bp deletion in *NbXLG4* (Fig. 2a), leading to a truncation of amino acids 30–41. However, *Nbxlg4*-L2 showed immune defect similar to those of *Nbxlg4-L1*, indicating that these 11 amino acids are important for the function of NbXLG4. Consistent with previous reports that XLG proteins are required for plant resistance against bacterial and fungal pathogens (Maruta et al. 2015; Liang et al. 2016; Urano et al. 2016; Zhao et al. 2022), here we showed that mutations in *NbXLG3/5* and *NbXLG4* resulted in severely impaired resistance to the bacterial pathogen *Pst* DC3000 and the fungal pathogen *S. sclerotiorum* (Fig. 3). To date, the role of XLG proteins in plant resistance to oomycete pathogens has not been investigated. Therefore, we challenged *Nbxlg* mutants with *P. capsici*, *P. infestans*, and *P. parasitica* and found that NbXLG3/5 and NbXLG4 are essential for plant resistance to these oomycete pathogens (Fig. 4). These findings are the first to show that XLG proteins are required for plant resistance to oomycete pathogens and may help to improve our understanding of the role of XLG proteins in plant immunity.

Next, we examined the functions of NbXLG3/5 and NbXLG4 in microbial pattern-induced immunity. The results showed that these three NbXLGs are required for flg22- or chitin-induced ROS burst and defense gene expression (Fig. 5). Consistent with the roles of XLGs in *Arabidopsis* and rice, NbXLG3, NbXLG4, and NbXLG5 interacted with NbGβ and were complexed with PRRs (NbFLS2 and NbCERK1) (Additional file 1: Figure S7). This result indicated that the XLG-Gβγ heterotrimers are involved in PRR complexes to regulate plant immune signaling. The role of NbGβ in plant immunity needs to be investigated in future studies. Intriguingly, we observed that transient expression of *AtXLGs* cannot restore the defect of *Nbxlg4* in flg22-induced ROS

(See figure on next page.)

Fig. 6 *Nbxlg3,5* mutant plants have enhanced resistance to abiotic stresses. **a** *Nbxlg3,5* mutant plants showed significantly enhanced resistance to salt and osmotic stresses. *Nicotiana benthamiana* seedlings were vertically grown on 1/2 MS medium supplemented with different concentrations of NaCl, mannitol, or PEG for 7 days. The seedlings were photographed and root length was measured. The related statistical data was shown in Additional file 1: Figure S8. **b** *Nbxlg4* mutant plants showed normal resistance to salt and osmotic stresses. *N. benthamiana* seedlings were vertically grown on 1/2 MS medium supplemented with different concentrations of NaCl, mannitol, or PEG for 7 days. The seedlings were photographed and root length was measured. The related statistical data was shown in Additional file 1: Figure S9

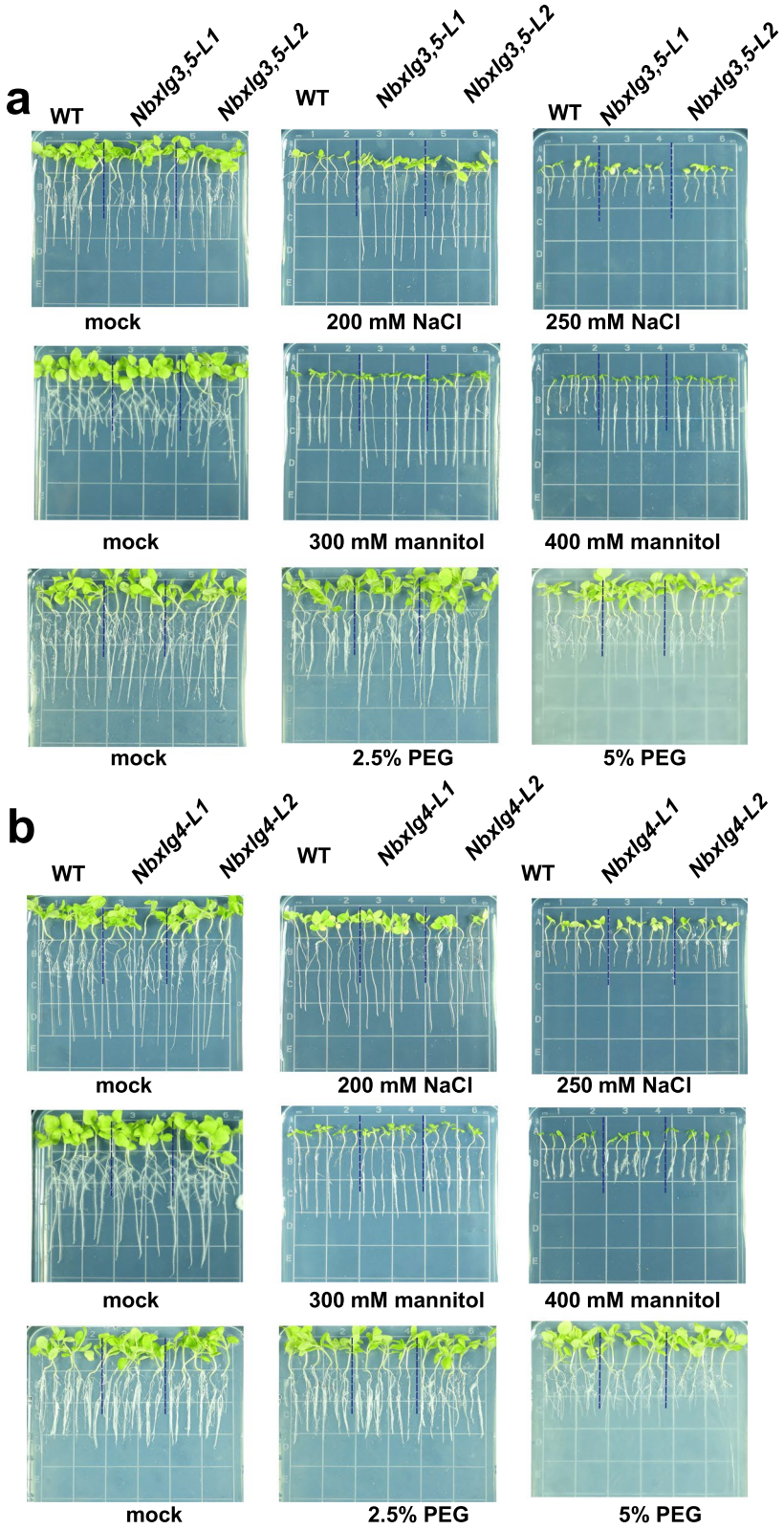

Fig. 6 (See legend on previous page.)

production and only partially restores the impaired ROS burst in *Nbxlg3,5* (Additional file 1: Figure S6).

Moreover, we showed that NbXLG3 and NbXLG5 negatively regulated plant resistance to salt and osmotic stresses. In contrast, AtXLGs are required for plant resistance to osmotic and salt stresses (Ding et al. 2008; Urano et al. 2016). The *Nbxlg3,5* mutant lines had significantly enhanced resistance to high-salt, mannitol, and PEG (Fig. 6). However, *Nbxlg4* mutant lines showed normal resistance to salt and osmotic stresses (Fig. 6). Thus, NbXLG3 and NbXLG5 can potentially improve plant resistance to biotic and abiotic stresses. Further studies are required to investigate the role of XLG proteins in plant resistance to biotic and abiotic stresses in other *Solanaceae* plants. It will also be worth studying the effect of XLG proteins on growth, development, and yield-related agronomic traits in *Solanaceae* plants such as tomatoes and potatoes.

Conclusions

In this study, we generated *Nbxlg3,5* and *Nbxlg4* knockout mutants and analyzed their immune phenotypes. *Nbxlg3,5* and *Nbxlg4* mutants showed severe defects in resistance against fungal and bacterial pathogens. We further demonstrated that XLG proteins are required for plant resistance to oomycete pathogens such as *P. capsici*, *P. infestans*, and *P. parasitica*. We revealed that NbXLG3/5 and NbXLG4 are involved in the immune receptor complex to regulate microbial patterns-induced immune responses. In addition, we demonstrated that the *Nbxlg3,5* mutant has enhanced resistance to salt and osmotic stresses. NbXLG3 and NbXLG5 potentially play an important role in the coordinated regulation of plant resistance to biotic and abiotic stresses and might be ideal targets for the improvement of plant adaption to environmental changes.

Methods

Plant materials and conditions

The *N. benthamiana* plants used for most of the experiments in this study were soil-grown at 23 °C under a 10-h light/14-h dark photoperiod. The *Nbxlg3,5* and *Nbxlg4* mutants were generated by CRISPR-Cas9 approach. The *N. benthamiana* plants used for osmotic stress assays were grown at 23 °C on 1/2 MS medium under a 14-h light/10-h dark photoperiod.

Bioinformatic analyses

Full-length protein sequences of G proteins were used for construction of the phylogenetic trees and the protein sequences were listed in Additional file 2: Table S1. Phylogenetic neighbor-Joining dendrograms were constructed using MEGA 11 software.

Plasmid construction and generation of *Nbxlg* mutant lines

To perform VIGS assay, a 200–300 bp fragment targeting *NbXLG1,6*, *NbXLG2,7*, *NbXLG3,5* or *NbXLG4* was amplified and cloned into pTRV2 vector. For LCI assay, the coding sequences of the target genes were amplified and cloned into pCAMBIA1300-35S-Cluc-RBS or pCAMBIA1300-35S-HA-Nluc-RBS vector. To perform Co-IP assays, the corresponding genes were amplified and inserted into pCAMBIA1300-35S-FLAG-RBS or pCAMBIA1300-35S-HA-RBS vector. To generate knockout lines of *NbXLGs*, a pair of guide RNAs targeting the corresponding gene were designed and cloned into pHEE401 vector (Wang et al. 2015). The constructs were then introduced into *N. benthamiana* plants by *Agrobacterium*-mediated transformation (Ellis et al. 1987). The primers used in this study are listed in Additional file 3: Table S2.

Virus-induced gene silencing (VIGS)

VIGS was performed as previously described (Liu et al. 2002). *A. tumefaciens* strains harboring the constructed TRV2 vector or TRV1 vector were resuspended in an infiltration solution (10 mmol/L $MgCl_2$, 10 mmol/L MES pH5.7, and 200 μM acetosyringone) to a final OD 600 of 1.0. Equal amount of *A. tumefaciens* with TRV1 or TRV2 was mixed and infiltrated into primary leaves of *N. benthamiana* during the four-leaf stage. TRV2:GFP and TRV2:PDS were used as negative and positive controls, respectively. The gene silencing efficiency was examined by qPCR analysis.

Pathogen infection assays

For bacterial inoculation assay, 4- to 5-week-old soil grown *N. benthamiana* plants were infiltrated with *Pst* DC3000 or *Pst* DC3000 *hrcC*$^-$ at a concentration of 1×10^5 CFU/mL. In planta bacterial titers were determined at 3 days post-inoculation (dpi).

For *P. capsici* infection assay, *P. capsici* strain LT263 was cultured at 25 °C on V8 agar plates for 2 days. Mycelial plugs were cultured in liquid V8 medium for 3 days, washed with sterilized water, and incubated in water to promote sporangia formation. To release the zoospores, the cultures were incubated at 4 °C for 40 min, followed by at 25 °C for 1 h. Detached *N. benthamiana* leaves were incubated with 150 zoospores and were kept in plastic boxes with high humidity in the dark. The leaves were photographed under UV light at 36–48 h post-inoculation (hpi). Lesion areas were measured and calculated by Image J software (Yu et al. 2012).

For *P. infestans* infection assay, the *P. infestans* strain TDT-88069 was cultured at 20 °C on Rye agar plates. The mycelium was flooded with water and scraped with a glass rod to release sporangia. Leaves were incubated with 350 sporangia and kept in plastic boxes with high humidity in the dark. The leaves were photographed under UV light at 7 dpi and lesion areas were measured by Image J software (Liang et al. 2021).

For *S. sclerotiorum* and *P. parasitica* infection assays, *N. benthamiana* leaves were inoculated with fresh mycelial plugs (5 mm in diameter). The leaves were put in a plastic box with high humidity and were photographed at 24 hpi (*S. sclerotiorum*) or 60 hpi (*P. parasitica*), and lesion areas were measured by Image J software (Huang et al. 2019; Nie et al. 2019).

Oxidative burst measurement

N. benthamiana leaf discs were collected and incubated overnight in a 96-well plate containing 200 µL water. The water was replaced with 200 µL reaction buffer containing 20 µM L-012 (Wako Chemical, Tokyo, Japan), 10 µg/mL horseradish peroxidase (Sigma), and 1 µM elicitors flg22 or 200 µg/mL chitin before measurement with a luminometer (Tecan F200) (Zhang et al. 2007).

Co-IP assay

The indicated constructs were expressed in *N. benthamiana* leaves by *Agrobacterium*-mediated transient expression system for 2 days. The leaves were collected and grounded in liquid nitrogen, and total protein was then extracted with protein extraction buffer [50 mM HEPES (pH 7.5), 150 mM KCl, 1 mM EDTA, 0.5% Trition-X 100, 1 mM DTT, proteinase inhibitor cocktail]. Total protein was incubated with anti-FLAG M2 agrose (Sigma) for 3 h, washed with protein extraction buffer for 6 times, and eluted with 3 × FLAG peptide (Sigma), and the immunoprecipitates were separated on SDS-PAGE gel. Protein interactions were detected with anti-HA and anti-FLAG immunoblots (Wang et al. 2020).

MAPK activity assay

N. benthamiana leaves were infiltrated with 1 µM flg22, 200 µg/mL chitin, or water. After incubation for 0, 8, and 16 min, samples were collected and ground in liquid nitrogen and resuspended in lysis buffer [50 mM HEPES (pH 7.5), 150 mM KCl, 1 mM EDTA, 0.5% Trition-X 100, 1 mM DTT, proteinase inhibitor cocktail]. Total proteins were separated on SDS-PAGE gel, and activation of MAPK was examined by anti-pERK immunoblots.

Luciferase complementation image (LCI) assay

The LCI assay was performed following the previously published protocol (Zhao and Zhou 2020). The indicated Cluc and Nluc constructs were expressed in *N. benthamiana* leaves by *Agrobacterium*-mediated transient expression. Leaf disks were taken at 2 days post-infiltration, incubated with 1 mM luciferin in a 96-well plate for 10–20 min, and the relative luminescence unit was measured by luminometer (Tecan).

RNA isolation and qPCR analysis

Four to five-week-old *N. benthamiana* plants were treated with 200 µg/mL chitin, 1 µM flg22, or water for 3 h. Total RNA was extracted using Eastep Supre RNA extraction Kit (Promega) following manufacturer's instructions. The first strand cDNA was synthesized with the SuperScriptIII First-Strand Kit (Invitrogen) and subjected to qPCR analysis. The indicated primers were listed in Additional file 3: Table S2.

Osmotic stress assays

The *N. benthamiana* seedlings were vertically grown on 1/2 MS medium at 23 °C under a 16-h day/8-h night cycle for 5 days. Then, the seedlings were transferred to 1/2 MS medium supplemented with different concentrations of NaCl, mannitol, or PEG and incubated for another 7 days. The plates were photographed and root length was measured (Farid et al. 2013).

Abbreviations

ABA: Abscisic acid; ET: Ethylene; GDP: Guanosine diphosphate; GPCR: G protein-coupled receptor; GTP: Guanosine triphosphate; MAPK: Mitogen-activated protein kinase; PEG: Polyethylene glycol; PRR: Pattern-recognition receptor; PTI: Pattern-triggered immunity; RK: Receptor kinase; RLK: Receptor-like kinase; RLP: Receptor-like protein; ROS: Reactive oxygen species; VIGS: Virus-induced gene silencing; XLG: Extra-large G protein.

Supplementary Information

The online version contains supplementary material available at https://doi.org/10.1186/s42483-022-00155-9.

Additional file 1: Figure S1. Alignment of XLG proteins from *Arabidopsis*, *Nicotiana benthamiana*, *Solanum lycopersicum*, and *Solanum tuberosum*. **Figure S2**. qPCR analysis of *NbXLG* gene silencing efficiency by virus-induced gene silencing (VIGS). **Figure S3**. Sequence verification of the mutation site in the *Nbxlg3,5* and *Nbxlg4* mutant lines. **Figure S4**. Verification of the Cas9-free mutant lines by PCR analysis. **Figure S5**. NbXLG3, NbXLG4, and NbXLG5 do not affect MAPK activation induced by flg22 (a) or chitin (b). **Figure S6**. *Arabidopsis* XLGs fail to restore the defect in flg22-induced ROS in *Nbxlg3,5* and *Nbxlg4*. **Figure S7**. NbXLGs interact with NbGβ and are involved in the immune receptor complex. **Figure S8**. *Nbxlg3,5* mutant lines showed enhanced resistance to abiotic stresses. **Figure S9**. *Nbxlg4* mutant lines showed normal resistance to abiotic stresses.

Additional file 2: Table S1. Gα Protein sequences used for construction of the phylogenetic tree.

Additional file 3: Table S2. Primers used in this study.

Acknowledgements

Not applicable.

Author contributions
XL and DD coordinated the research and wrote the paper. YL performed majority of the experiments. QZ, LG, JK, XW, GX, and XC contributed to plasmid construction and pathogen infection assays. All authors read and approved the final manuscript.

Funding
The work was supported by grants from the Chinese Natural Science Foundation (32270282), the open competition program of top ten critical priorities of Agricultural Science and Technology Innovation for the 14th Five-Year Plan of Guangdong Province (2022SDZG07), and Double First-class Discipline Promotion Project (2021B10564001).

Availability of data and materials
The datasets used and/or analyzed during the current study are available from the corresponding author on reasonable request.

Declarations

Ethics approval and consent to participate
Not applicable.

Consent for publication
Not applicable.

Competing interests
The authors declare that they have no competing interests.

Author details
[1]College of Plant Protection, China Agricultural University, Beijing 100193, China. [2]State Key Laboratory for Conservation and Utilization of Subtropical Agro-Bioresources, College of Life Sciences, South China Agricultural University, Guangzhou 510642, China. [3]College of Plant Protection, Nanjing Agricultural University, Nanjing 210095, China.

Received: 6 October 2022 Accepted: 9 December 2022
Published online: 23 December 2022

References

Bommert P, Je BI, Goldshmidt A, Jackson D. The maize Gα gene *COMPACT PLANT2* functions in CLAVATA signalling to control shoot meristem size. Nature. 2013;502(7472):555–8. https://doi.org/10.1038/nature12583.

Cao Y, Liang Y, Tanaka K, Nguyen CT, Jedrzejczak RP, Joachimiak A, et al. The kinase LYK5 is a major chitin receptor in *Arabidopsis* and forms a chitin-induced complex with related kinase CERK1. eLife. 2014;3:e03766. https://doi.org/10.7554/eLife.03766.

Chinchilla D, Bauer Z, Regenass M, Boller T, Felix G. The *Arabidopsis* receptor kinase FLS2 binds flg22 and determines the specificity of flagellin perception. Plant Cell. 2006;18(2):465–76. https://doi.org/10.1105/tpc.105.036574.

Chinchilla D, Zipfel C, Robatzek S, Kemmerling B, Nürnberger T, Jones JD, et al. A flagellin-induced complex of the receptor FLS2 and BAK1 initiates plant defence. Nature. 2007;448(7152):497–500. https://doi.org/10.1038/nature05999.

Choudhury SR, Pandey S. Phosphorylation-dependent regulation of G-protein cycle during nodule formation in soybean. Plant Cell. 2015;27(11):3260–76. https://doi.org/10.1105/tpc.15.00517.

DeFalco TA, Zipfel C. Molecular mechanisms of early plant pattern-triggered immune signaling. Mol Cell. 2021;81(17):3449–67. https://doi.org/10.1016/j.molcel.2021.07.029.

Ding L, Pandey S, Assmann SM. *Arabidopsis* extra-large G proteins (XLGs) regulate root morphogenesis. Plant J. 2008;53(2):248–63. https://doi.org/10.1111/j.1365-313X.2007.03335.x.

Ellis JG, Llewellyn DJ, Dennis ES, Peacock WJ. Maize *Adh-1* promoter sequences control anaerobic regulation: addition of upstream promoter elements from constitutive genes is necessary for expression in tobacco. EMBO J. 1987;6(1):11–6. https://doi.org/10.1002/j.1460-2075.1987.tb04711.x.

Fan C, Xing Y, Mao H, Lu T, Han B, Xu C, et al. *GS3*, a major QTL for grain length and weight and minor QTL for grain width and thickness in rice, encodes a putative transmembrane protein. Theor Appl Genet. 2006;112(6):1164–71. https://doi.org/10.1007/s00122-006-0218-1.

Farid A, Malinovsky FG, Veit C, Schoberer J, Zipfel C, Strasser R. Specialized roles of the conserved subunit OST3/6 of the oligosaccharyltransferase complex in innate immunity and tolerance to abiotic stresses. Plant Physiol. 2013;162(1):24–38. https://doi.org/10.1104/pp.113.215509.

Fujisawa Y, Kato T, Ohki S, Ishikawa A, Kitano H, Sasaki T, et al. Suppression of the heterotrimeric G protein causes abnormal morphology, including dwarfism, in rice. Proc Natl Acad Sci U S A. 1999;96(13):7575–80. https://doi.org/10.1073/pnas.96.13.7575.

Huang X, Qian Q, Liu Z, Sun H, He S, Luo D, et al. Natural variation at the *DEP1* locus enhances grain yield in rice. Nat Genet. 2009;41(4):494–7. https://doi.org/10.1038/ng.352.

Huang G, Liu Z, Gu B, Zhao H, Jia J, Fan G, et al. An RXLR effector secreted by *Phytophthora parasitica* is a virulence factor and triggers cell death in various plants. Mol Plant Pathol. 2019;20(3):356–71. https://doi.org/10.1111/mpp.12760.

Lee YR, Assmann SM. *Arabidopsis thaliana* "extra-large GTP-binding protein" (AtXLG1): a new class of G-protein. Plant Mol Biol. 1999;40(1):55–64. https://doi.org/10.1023/a:1026483823176.

Liang X, Ding P, Lian K, Wang J, Ma M, Li L, et al. *Arabidopsis* heterotrimeric G proteins regulate immunity by directly coupling to the FLS2 receptor. eLife. 2016;5:e13568. https://doi.org/10.7554/eLife.13568.

Liang X, Ma M, Zhou Z, Wang J, Yang X, Rao S, et al. Ligand-triggered de-repression of *Arabidopsis* heterotrimeric G proteins coupled to immune receptor kinases. Cell Res. 2018;28(5):529–43. https://doi.org/10.1038/s41422-018-0027-5.

Liang X, Bao Y, Zhang M, Du D, Rao S, Li Y, et al. A *Phytophthora capsici* RXLR effector targets and inhibits the central immune kinases to suppress plant immunity. New Phytol. 2021;232(1):264–78. https://doi.org/10.1111/nph.17573.

Liu Y, Schiff M, Marathe R, Dinesh-Kumar SP. Tobacco *Rar1*, *EDS1* and *NPR1/NIM1* like genes are required for *N*-mediated resistance to tobacco mosaic virus. Plant J. 2002;30(4):415–29. https://doi.org/10.1046/j.1365-313x.2002.01297.x.

Liu J, Ding P, Sun T, Nitta Y, Dong O, Huang X, et al. Heterotrimeric G proteins serve as a converging point in plant defense signaling activated by multiple receptor-like kinases. Plant Physiol. 2013;161(4):2146–58. https://doi.org/10.1104/pp.112.212431.

Ma M, Wang W, Fei Y, Cheng HY, Song B, Zhou Z, et al. A surface-receptor-coupled G protein regulates plant immunity through nuclear protein kinases. Cell Host Microbe. 2022;30(11):1602–14. https://doi.org/10.1016/j.chom.2022.09.012.

Maruta N, Trusov Y, Brenya E, Parekh U, Botella JR. Membrane-localized extra-large G proteins and Gβγ of the heterotrimeric G proteins form functional complexes engaged in plant immunity in *Arabidopsis*. Plant Physiol. 2015;167(3):1004–16. https://doi.org/10.1104/pp.114.255703.

Miao J, Yang Z, Zhang D, Wang Y, Xu M, Zhou L, et al. Mutation of *RGG2*, which encodes a type B heterotrimeric G protein γ subunit, increases grain size and yield production in rice. Plant Biotechnol J. 2019;17(3):650–64. https://doi.org/10.1111/pbi.13005.

Nie J, Yin Z, Li Z, Wu Y, Huang L. A small cysteine-rich protein from two kingdoms of microbes is recognized as a novel pathogen-associated molecular pattern. New Phytol. 2019;222(2):995–1011. https://doi.org/10.1111/nph.15631.

Oldham WM, Hamm HE. Heterotrimeric G protein activation by G-protein-coupled receptors. Nat Rev Mol Cell Biol. 2008;9(1):60–71. https://doi.org/10.1038/nrm2299.

Pandey S. Heterotrimeric G-protein signaling in plants: conserved and novel mechanisms. Annu Rev Plant Biol. 2019;70:213–38. https://doi.org/10.1146/annurev-arplant-050718-100231.

Pandey S, Monshausen GB, Ding L, Assmann SM. Regulation of root-wave response by extra large and conventional G proteins in *Arabidopsis thaliana*. Plant J. 2008;55(2):311–22. https://doi.org/10.1111/j.1365-313X.2008.03506.x.

Stateczny D, Oppenheimer J, Bommert P. G protein signaling in plants: minus times minus equals plus. Curr Opin Plant Biol. 2016;34:127–35. https://doi.org/10.1016/j.pbi.2016.11.001.

Sun H, Qian Q, Wu K, Luo J, Wang S, Zhang C, et al. Heterotrimeric G proteins regulate nitrogen-use efficiency in rice. Nat Genet. 2014;46(6):652–6. https://doi.org/10.1038/ng.2958.

Ueguchi-Tanaka M, Fujisawa Y, Kobayashi M, Ashikari M, Iwasaki Y, Kitano H, et al. Rice dwarf mutant *d1*, which is defective in the α subunit of the heterotrimeric G protein, affects gibberellin signal transduction. Proc Natl Acad Sci U S A. 2000;97(21):11638–43. https://doi.org/10.1073/pnas.97.21.11638.

Urano D, Maruta N, Trusov Y, Stoian R, Wu Q, Liang Y, et al. Saltational evolution of the heterotrimeric G protein signaling mechanisms in the plant kingdom. Sci Signal. 2016;9(446):ra93. https://doi.org/10.1126/scisignal.aaf9558.

Utsunomiya Y, Samejima C, Fujisawa Y, Kato H, Iwasaki Y. Rice transgenic plants with suppressed expression of the β subunit of the heterotrimeric G protein. Plant Signal Behav. 2012;7(4):443–6. https://doi.org/10.4161/psb.19378.

Wang ZP, Xing HL, Dong L, Zhang HY, Han CY, Wang XC, et al. Egg cell-specific promoter-controlled CRISPR/Cas9 efficiently generates homozygous mutants for multiple target genes in *Arabidopsis* in a single generation. Genome Biol. 2015;16(1):144. https://doi.org/10.1186/s13059-015-0715-0.

Wang D, Liang X, Bao Y, Yang S, Zhang X, Yu H, et al. A malectin-like receptor kinase regulates cell death and pattern-triggered immunity in soybean. EMBO Rep. 2020;21(11):e50442. https://doi.org/10.15252/embr.202050442.

Wang Y, Zhang H, Wang P, Zhong H, Liu W, Zhang S, et al. *Arabidopsis* EXTRA-LARGE G PROTEIN 1 (XLG1) functions together with XLG2 and XLG3 in PAMP-triggered MAPK activation and immunity. J Integr Plant Biol. 2022. https://doi.org/10.1111/jipb.13391.

Wu Q, Regan M, Furukawa H, Jackson D. Role of heterotrimeric Gα proteins in maize development and enhancement of agronomic traits. PLoS Genet. 2018;14(4):e1007374. https://doi.org/10.1371/journal.pgen.1007374.

Yu X, Tang J, Wang Q, Ye W, Tao K, Duan S, et al. The RxLR effector Avh241 from *Phytophthora sojae* requires plasma membrane localization to induce plant cell death. New Phytol. 2012;196(1):247–60. https://doi.org/10.1111/j.1469-8137.2012.04241.x.

Yu Y, Chakravorty D, Assmann SM. The G Protein *β*-Subunit, AGB1, interacts with FERONIA in RALF1-regulated stomatal movement. Plant Physiol. 2018;176(3):2426–40. https://doi.org/10.1104/pp.17.01277.

Zhang J, Shao F, Li Y, Cui H, Chen L, Li H, et al. A *Pseudomonas syringae* effector inactivates MAPKs to suppress PAMP-induced immunity in plants. Cell Host Microbe. 2007;1(3):175–85. https://doi.org/10.1016/j.chom.2007.03.006.

Zhao Y, Zhou JM. Luciferase complementation assay for detecting protein interactions. Chin Bull Bot. 2020;55(01):69–75. https://doi.org/10.11983/CBB19229. (**in Chinese**).

Zhao Y, Shi Y, Jiang G, Wu Y, Ma M, Zhang X, et al. Rice extra-large G proteins play pivotal roles in controlling disease resistance and yield-related traits. New Phytol. 2022;234(2):607–17. https://doi.org/10.1111/nph.17997.

Zhu H, Li GJ, Ding L, Cui X, Berg H, Assmann SM, et al. *Arabidopsis* extra large G-protein 2 (XLG2) interacts with the Gβ subunit of heterotrimeric G protein and functions in disease resistance. Mol Plant. 2009;2(3):513–25. https://doi.org/10.1093/mp/ssp001.

Ready to submit your research? Choose BMC and benefit from:

- fast, convenient online submission
- thorough peer review by experienced researchers in your field
- rapid publication on acceptance
- support for research data, including large and complex data types
- gold Open Access which fosters wider collaboration and increased citations
- maximum visibility for your research: over 100M website views per year

At BMC, research is always in progress.

Learn more biomedcentral.com/submissions

BMC